Heat Transfer Engineering

ISSN: 0145-7632 (Print) 1521-0537 (Online) Journal homepage: http://www.tandfonline.com/loi/uhte20

Influence of Fouling Biofilms on Heat Transfer

W. G. CHARACKLIS , M. J. NEVIMONS & B. F. PICOLOGLOU

To cite this article: W. G. CHARACKLIS , M. J. NEVIMONS & B. F. PICOLOGLOU (1981) Influence of Fouling Biofilms on Heat Transfer, Heat Transfer Engineering, 3:1, 23-37, DOI: 10.1080/01457638108939572

To link to this article: http://dx.doi.org/10.1080/01457638108939572

Published online: 27 Mar 2007.

Influence of Fouling Biofilms on Heat Transfer

W. G. CHARACKLIS
School of Engineering, Montana State University, Bozeman, Montana 59717

M. J. NIMMONS
Assistant Project Engineer, D'Appolonia Consulting Engineers, Inc., Irvine, California 92714

B. F. PICOLOGLOU
Engineer, Argonne National Laboratory, Argonne, Illinois 60439

In heat exchange equipment, fouling biofilm formation causes a significant energy loss by increasing heat transfer resistance. This paper describes experiments which quantify the influence of fouling biofilms on heat transfer resistance under controlled laboratory conditions. Experimental results compare well with a rather simple mathematical model employing friction factor, biofilm thickness, wall temperature, bulk temperature, and fluid properties as inputs. Limitations of the experimental apparatus and mathematical model are discussed.

INTRODUCTION

Biofouling in heat exchangers causes pronounced increases in fluid frictional resistance [1] and heat transfer resistance [2]. The energy losses that result are of major concern in power generation and in the chemical process industry.

Biofouling is a general term referring to undesirable effects due to attachment of microorganisms at liquid-solid interfaces. The microorganisms produce a slime layer. When this slime layer is formed on the inside surface of heat exchange tubes, it causes increased heat transfer resistance and fluid frictional resistance which results in energy losses.

The laboratory research was conducted at Rice University, Houston, Texas. The authors gratefully acknowledge partial financial support from the National Science Foundation (ENG 77-20934), the Electric Power Research Institute (RP 902-1), the Office of Naval Research (N00014-80-C-0475), and Calgon Corporation. Ms. Sharlene Vehnekamp prepared the manuscript. M. Turakhia, Dr. W. E. Genetti, Dr. J. G. Knudsen, and Dr. L. V. McIntire provided helpful advice.

Biofouling is particularly acute in industrial cooling water systems. Over a 7-week period, Purkiss [2] observed almost 80% decrease in the performance of a cooling system due to biofouling. Fouling resistance, in six power plant condensers of 240 MW design capacity, was 0.97 $m^2\ ^\circ C\ kW^{-1}$ [3]. The cost of extra fuel annually was estimated at $350,000 (1976 dollars).

Biofouling is not limited to microbial activity. The term includes the interaction of the microorganisms and the slime layer with the chemistry of both the solid surface and the bulk fluid. The interaction can enhance some of the more commonly known fouling phenomena, such as precipitation or crystallization (scaling) and corrosion. The rate and extent of fouling will be determined partially by the physical and transport properties of the fouling films that result (e.g., thermal conductivity, rheological properties, roughness).

Relatively little effort has been invested in mechanistic studies relating biofilm development to heat transfer resistance. Kirkpatrick et al. [4]

have developed a mathematical model describing heat transfer and mass transfer for a fluid flowing in a tube in which a biofilm is developing. The Ocean Thermal Energy Conversion (OTEC) program has accumulated field data that is of limited use due to its empirical nature. Our work was undertaken to provide a more fundamental framework for understanding the influence of biofouling on heat transfer resistance.

The purpose of this study was to explore the process of biofouling and its influence on heat transfer resistance. This paper will be concerned only with microbial slime layers and, therefore, the term "biofouling" will be used for microbial fouling, and the term "biofilm" for the microbial slime layer.

MATHEMATICAL DESCRIPTION OF THE PROBLEM

The objective of this study was to determine the influence of biofilm development on heat transfer in turbulent flow. The following model provides a systematic basis for interpreting the results of the study.

Figure 1 shows a circular tube which is being heated at a constant rate. A biofilm is developing on the inside of the tube wall. The rate of heat flow from the cylinder to the bulk fluid is expressed as follows:

$$dQ = U(2\pi r_I\, dz)(T_i - T_b) \tag{1}$$

The overall heat transfer coefficient is defined as follows:

$$U_{\text{calc}} = \left[\frac{1}{h} + \frac{r_I \ln (r_1/r_I)}{k_B} + \frac{r_I \ln (r_i/r_1)}{k_{\text{tube}}}\right]^{-1} \tag{2}$$

The convective heat transfer coefficient is defined by:

$$h = \frac{dQ}{2\pi r_I (T_I - T_b)\, dz} \tag{3}$$

In a clean system (i.e., no biofilm), the second term in Eq. (2) goes to zero. As biofilm develops, the overall heat transfer coefficient changes. If the change in $T_i - T_b$ is insignificant with longitudinal distance L, the integration of Eq. (1) over the length of the heated section gives the following:

$$\frac{Q}{A_I} = \left[\frac{1}{h} + \frac{r_I \ln (r_1/r_I)}{k_B} + \frac{r_I \ln (r_i/r_1)}{k_{\text{tube}}}\right]^{-1} \times (T_i - T_b) \tag{4}$$

The thermal conductivity of the biofilm k_B can be determined by measuring the overall heat transfer coefficient U at a constant heat flux if k_{tube} and h have been determined.

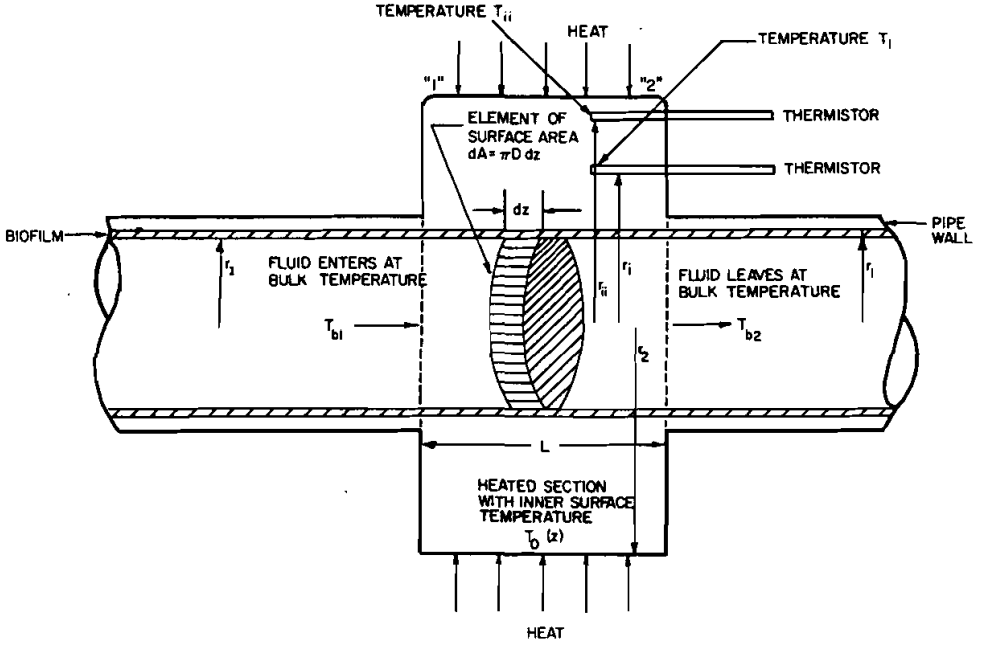

Figure 1 Physical basis for modeling heat transfer in a circular tube with fouling biofilm.

Convective Heat Transfer Coefficient

The convective heat transfer coefficient can be determined by measuring the temperature differential between the biofilm–fluid interface and the bulk fluid. Such an effort is presently impractical due to difficulties in making accurate, nondisruptive temperature measurements at the biofilm–fluid interface. The relationship, however, between momentum transfer and heat transfer in turbulent flow provides an alternate means of determining the convective heat transfer coefficient.

Colburn [5] analyzed data on convective heat transfer and pressure drop from a large number of experiments and found it possible to predict the heat transfer coefficient from the friction factor. Expressed in terms of the Stanton number, the Colburn relationship is:

$$\mathrm{St}_b\ \mathrm{Pr}_f^{2/3} = \frac{f}{8} \tag{5}$$

The Stanton number is based on properties of the fluid at bulk temperature while the Prandtl number and friction factor are based on properties evaluated at the arithmetic mean of the bulk temperature and the temperature at the fluid–"solid" interface. The solid may be the clean tube surface or the biofilm. The Colburn relationship applies to flows with Reynolds numbers in excess of 10,000, and may be applied as an approximation in hydraulically rough tubes [4]. Equation (5) may be rearranged as follows:

$$h = 0.125 f C_p^{0.33} \mu^{-0.67} k^{0.67} \rho v_m \tag{6}$$

Consequently, the convective heat transfer coefficient h can be determined from fluid properties, fluid velocity, and friction factor data.

Overall Heat Transfer Coefficient

A steady state heat balance on a differential element of the heated tube (Fig. 1) results in the following:

$$\frac{d(rq_r)}{dr} = 0 \tag{7}$$

where

$$q_r = \frac{dQ}{dA} = \text{heat flux in } -r \text{ direction } (Mt^{-3})$$

Equation (7) can be expressed as follows:

$$\frac{d}{dr}\left(rk_{\text{tube}}\frac{dT}{dr}\right) = 0 \tag{8}$$

Boundary conditions are as follows:

$$\text{at } r = r_2, \quad q_2 = k_{\text{tube}}\frac{dT}{dr}$$

$$\text{at } r = r_1, \quad T = T_1$$

The solution of Eq. (8) with the boundary conditions yields the following:

$$T - T_1 = \frac{r_2 q_2}{k_{\text{tube}}} \ln\frac{r}{r_1} \tag{9}$$

The tube-wall temperature T_1 is difficult to measure but it is related to the bulk fluid temperature as follows:

$$k\frac{dT}{dr}\bigg|_{r=r_1} = U_{\text{meas}}(T_1 - T_b) = q_2 \tag{10}$$

Since

$$2\pi r_2 L q_2 = 2\pi r_1 L(T_1 - T_b)U_{\text{meas}}$$

Then

$$T_1 = \frac{q_2 r_2}{U_{\text{meas}} r_1} + T_b \tag{11}$$

Combining Eqs. (11) and (9) yields

$$T - T_b = r_2 q_2\left[\frac{1}{k_{\text{tube}}}\ln\frac{r}{r_1} + \frac{1}{U_{\text{meas}} r_1}\right] \tag{12}$$

Thus by measuring temperatures at two radial positions within the tube wall (r_{i} and r_{ii}), the effective heat flux (q_2) at the tube outer radius (r_2) can be obtained as follows:

$$q_2 = \frac{k_{\text{tube}}(T_{\text{ii}} - T_{\text{i}})}{r_2 \ln(r_{\text{i}}/r_{\text{ii}})} \tag{13}$$

Having obtained the heat flux q_2, the overall heat transfer coefficient U can be determined by measuring the bulk fluid temperature T_b and either T_{i} or T_{ii}. Solving Eq. (12) for U_{meas},

$$U_{\text{meas}}^{-1} = \left[(T_{\text{i}} - T_b) - \frac{r_2 q_2}{k_{\text{tube}}}\ln\frac{r_{\text{i}}}{r_1}\right]\frac{r_1}{r_2 q_2} \tag{14}$$

Changes in U_{meas} may be computed as biofilm develops by monitoring T_i, T_{ii}, and T_b and maintaining a constant heat flux.

This procedure was used experimentally to verify the model and to describe changes in heat transfer due to biofilm development.

EXPERIMENTAL

Experimental System

A diagram of the experimental system is presented in Fig. 2. The system consists of a continuous fermenter (chemostat) and an external tubular recycle loop. The dilution flow rate through the chemostat F_D is much smaller than the recycle flow rate F_R (i.e., $F_D \ll F_R$). Advantages of this system for laboratory experimentation include the following:

1. At the high recycle rates utilized, no longitudinal concentration gradients exist in the tubular recycle loop. The entire system is a continuous stirred tank reactor (CSTR). This simplifies the sampling and mathematics used in data interpretation. This system also minimizes water and microbial nutrient usage.
2. A short, mean-residence time can be maintained which minimizes biomass activity in the bulk fluid. Thus, the microbial activity is restricted to the reactor surfaces.
3. Fluid shear stress and convective heat transfer at the wall are independent of mean residence time in the reactor.

Other investigators have used a similar system but have not incorporated heat transfer processes [1].

The entire system is operated as a CSTR or a chemostat. Sterile glucose and trypticase soy broth (TSB) in a 1:1 weight ratio are fed into the fermenter from stock solutions. Air is continuously diffused into the fermenter. The nutrients are diluted by tap water flowing from a head tank. Experiments were initiated by inoculating the reactor with a heterogeneous microbial inoculum and operating in a batch mode for 6–8 h. Initial nutrient concentration for the batch period was 100 mg/L (1:1 weight ratio of glucose and TSB). Details of the experimental system and operating procedure can be found in [6].

The experimental system illustrated in Fig. 2 consists of five major components:

1. Fermenter
2. Test heat exchanger or thick-walled heat exchanger (TWHE)
3. Biofilm test section
4. Pressure drop reactor
5. Short heat exchanger

The characteristics and important dimensions of these components are presented in Table 1.

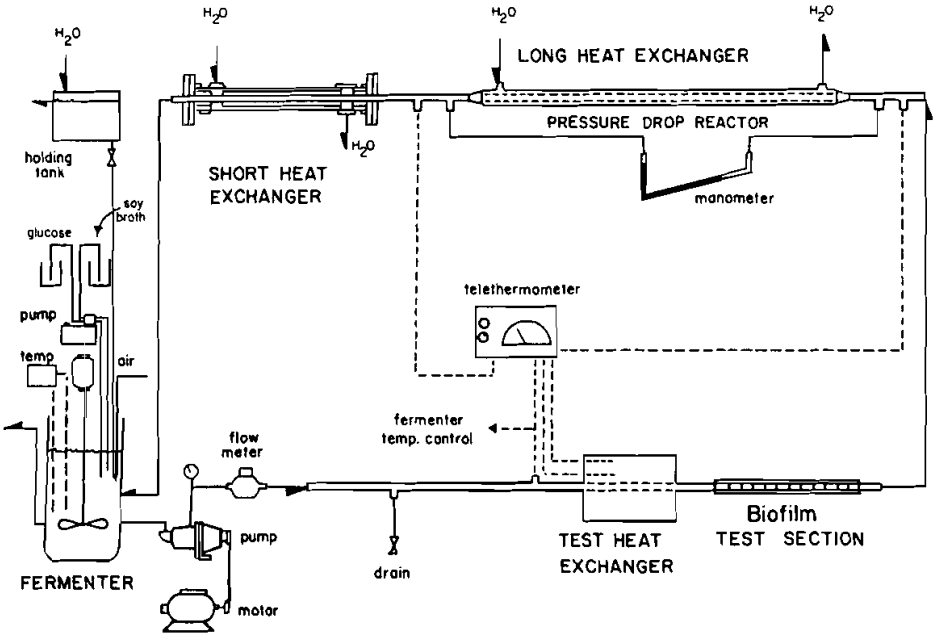

Figure 2 Diagram of experimental system.

Table 1 Characteristics and Important Dimensions of the Experimental System

Characteristic	Dimension
Overall system	
Operating volume	5670 cm^3
Wetted surface area	6950 cm^2
Fermenter	
Material of construction	Glass
Operating volume	2572 cm^3
Wetted surface area	746 cm^2
Thick-walled heat exchanger	
Material of construction	6061-T6 aluminum
Length	13.1 cm
Inside diameter	1.31 cm (1.39 after expt. 4)
Outside diameter	13.97 cm
Biofilm test section	
Material of construction	304 stainless steel
Length	39.4 cm
Inside diameter	1.98 cm
Outside diameter	2.22 cm
Sample tubes within test section	
Material of construction	304 stainless steel
Number within test section	8
Length	5.1 cm
Inside diameter	1.66 cm
Outside diameter	1.91 cm
Pressure drop section	
Material of construction	304 stainless steel
Length	329 cm
Inside diameter	1.66 cm
Outside diameter	1.91 cm
Length between pressure taps	310 cm
Short heat exchanger	
Material of construction	304 stainless steel
Length	99 cm
Inside diameter	1.66 cm
Outside diameter	1.91 cm

Thick-Walled Heat Exchanger (TWHE)

The change in heat transfer resistance due to biofilm development is measured in the TWHE. A diagram of the TWHE is presented in Fig. 3. Heat was supplied by a silicone rubber electrical heater bonded to the outside surface. Temperature was measured by two thermostats located at 1.37 and 6.48 cm from the center of the cylinder. The entire exchanger was heavily insulated.

Biofilm Test Section

The biofilm test section contained small removable sample tubes used for determining biofilm thickness. A similar test section was described by Picologlou et al. [1]. Eight sample tubes, placed end to end, were contained within the test section which constituted the sleeve. The test section was heated by a tube furnace to provide an inner surface temperature on the sample tubes equal to that in the TWHE.

Pressure Drop Reactor

The pressure drop was measured across this heated section of tube to provide a measure of the fluid frictional resistance within the recycle loop. The section was heated on the shell side by hot water to maintain an inner tube surface temperature equal to that in the TWHE and biofilm test section. Pressure drop was measured by an inclined mercury manometer.

Short Heat Exchanger

The short heat exchanger was used for cooling, whenever necessary, to maintain the bulk fluid temperature constant.

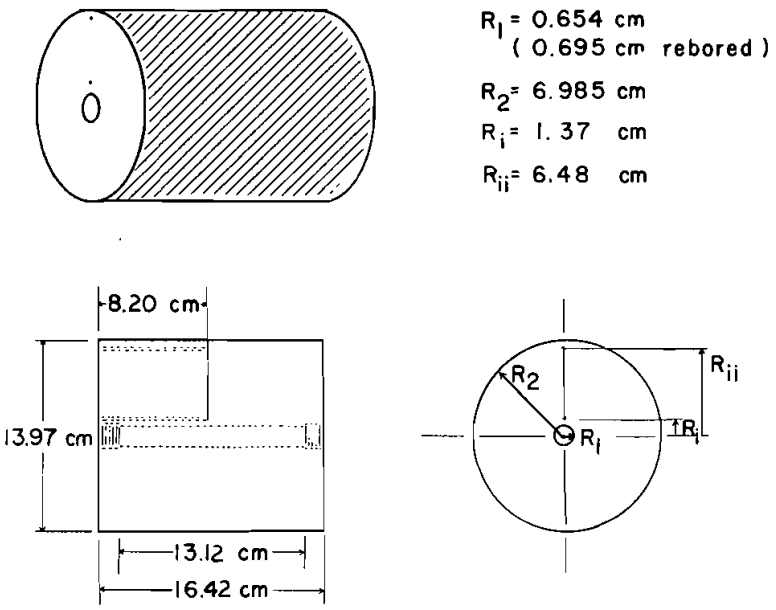

Figure 3 Diagram of thick-walled heat exchanger (TWHE).

Experimental Methods

Biofilm Thickness and Density

Biofilm volume was determined by measuring displacement of sample tubes with and without biofilm accumulation [1, 7]. Sample tube surface area was known and biofilm thickness was calculated. The estimated precision of the thickness measurement in this study was ±15 μm. After the volume was measured, the sample tube with the biofilm accumulation was dried and weighed. The sample tube was then cleaned, dried, and reweighed to determine the biofilm mass. Knowing the mass and volume, the biofilm density can be calculated.

Temperature Sensing

Temperature was measured with thermistors (accuracy to ±0.3°C) and monitored by a telethermometer with a resolution of 0.01°C. The system for maintaining desired temperatures in different components within the system is described in [6].

RESULTS

Table 2 presents a summary of experimental conditions and relevant results. The thermal power was maintained constant at approximately 350 W through all the experiments. The pressure drop (and, therefore, shear stress at the wall) was maintained constant and changes in flow rate were monitored to determine frictional resistance.

Biofilm Development

Biofilm thickness in these experiments was measured in the biofilm test section and increased in a

Table 2 Summary of Experimental Results

Experiment	T_b, °C	Initial shear stress, N/m^2	v_m, m/s	f_{max}	Th_{max}, μm	ρ_f, kg/m^3	Glucose loading rate, g/m^2 min^{-1}	F_D, L/min	k_B, W/m °C
1	31.9	2.20	0.809	0.067	245	39.9	682	0.474	0.70
2	31.5	2.28	0.807	0.092	94	18.3	68	0.474	0.71
3	31.5	2.28	0.805	0.037	94	14.4	34	0.474	–
6	28.3	2.28	0.807	0.208	141	16.2	68	0.474	0.68
7	26.7	2.30	0.807	0.154	259	28.0	171	0.474	0.52
8	26.7	2.28	0.808	0.212	232	23.6	68	0.474	0.70
9	28.3	2.28	0.807	0.202	128	24.0	68	0.474	0.58
10	31.5	2.28	0.808	0.030	0	0	0	0.474	No biofilm

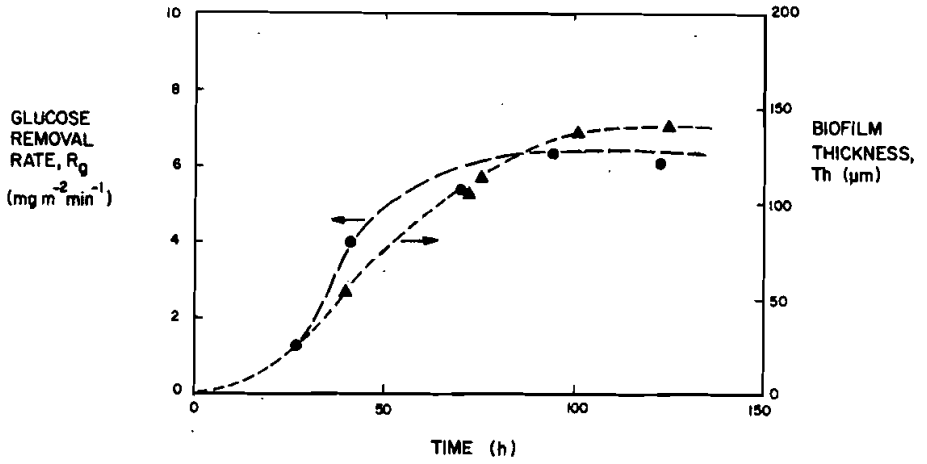

Figure 4 Progression of biofilm thickness and glucose removal rate during a typical experiment.

sigmoidal manner as indicated by Fig. 4. Others have observed the same characteristic progression [1, 8, 9]. Biofilm thickness within the plateau region ranged from 94 to 300 μm. The biofilm accumulation occurs at the expense of nutrients. The nutrient (glucose) removal rate also increases sigmoidally during an experiment (Fig. 4). Biofilm development rate increases with increasing glucose concentration and loading rate as evidenced by Fig. 5.

Biofilm Properties

Density

Biofilm density ranged from 15 to 40 mg/cm^{-3}. Higher substrate loadings have been observed to increase biofilm density [8, 9, 10], and this trend was observed in this experiment.

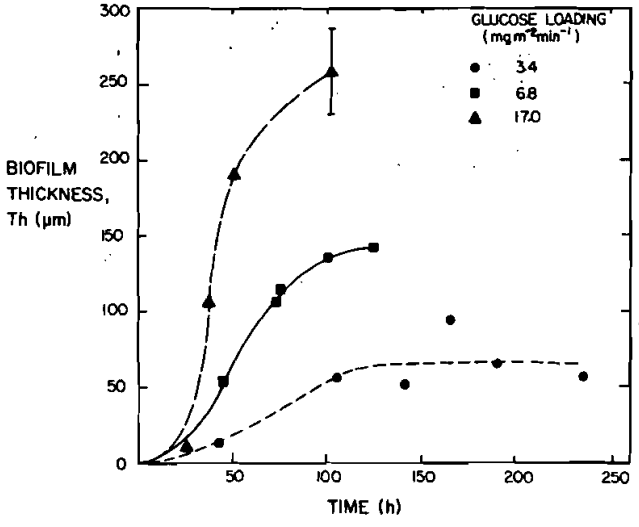

Figure 5 Influence of glucose loading rate on fouling biofilm development.

Thermal Conductivity

The thermal conductivity of the biofilm k_B may be derived by rearranging Eq. (2) in which U_{calc} has been replaced by U_{meas}:

$$k_B = \left[\frac{hk_{tube} - U_{meas}k_{tube} - U_{meas}hr_I \ln (r_i/r_1)}{U_{meas}hk_{tube}r_I \ln (r_1/r_I)}\right]^{-1} \quad (15)$$

By measuring biofilm thickness ($Th = r_1 - r_I$), the overall heat transfer coefficient, and the friction factor, k_B can be determined. Table 3 presents results of k_B determinations, and indicates that k_B is not significantly different from the thermal conductivity of water.

There was no significant correlation between k_B and biofilm density.

Table 3 Thermal Conductivity of Biofilm

Experiment	Biofilm thermal conductivity k_B, (W/m^{-1} °C)	Bulk temperature T_b, °C
1	0.7 ± 0.4 (3)†	31.9 ± 0.5
2	0.7 ± 0.1 (3)	31.50 ± 0.03
6	0.7 ± 0.2 (5)	28.30 ± 0.03
7	0.5 ± 0.2 (3)	26.70 ± 0.03
8	0.7 ± 0.4 (5)	26.70 ± 0.03
9	0.6 ± 0.1 (5)	28.30 ± 0.03
Grand mean	0.6 ± 0.2 (24)	
Water*	0.61	26.7
	0.62	32.2

*From [11].

†Numbers in parentheses refer to number of determinations.

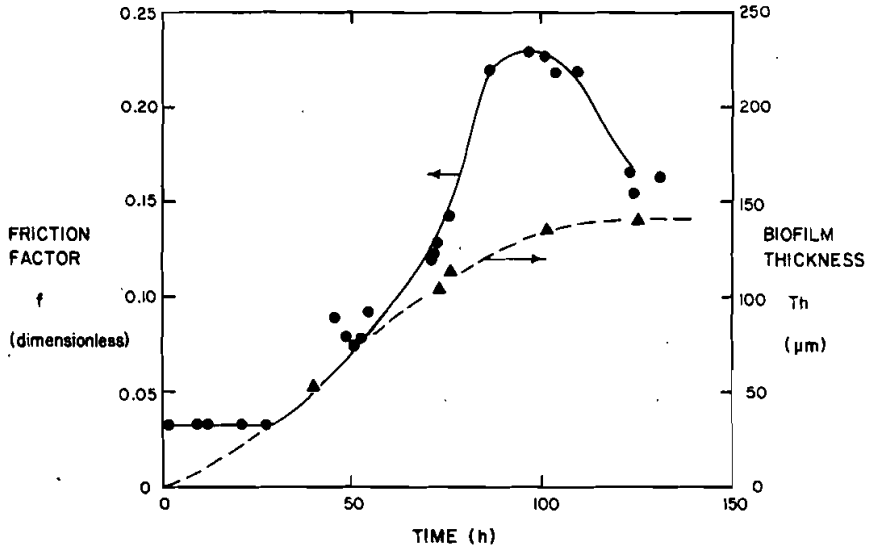

Figure 6 Progression of biofilm thickness and friction factor during a typical experiment.

Frictional Resistance

Frictional resistance is conveniently expressed by a dimensionless friction factor. In these experiments, v_m was maintained at 80.2 cm/s (2.6 fps) in the pressure drop section, and the change in Δp was monitored across a length of 329 cm. After an initial period of no change, the friction factor f increased with increased biofilm thickness (Fig. 6). The cause for increased f has been discussed in detail [1]. The friction factor increases more rapidly as glucose concentration and loading rate increases. The increase in f is sometimes followed by a dramatic decrease observable in experiments with high glucose loading rate (Fig. 7).

Overall Heat Transfer Resistance

Overall heat transfer resistance is conveniently expressed by the reciprocal of the overall heat transfer coefficient, U_{meas}^{-1}, defined by Eq. (14). U_{meas} was determined from measurements of T_i, T_b, and power input. Power input was maintained at 350 W for all experiments, so heat flux on the outside wall was approximately 4.86 kW/m^{-2}.

Observed heat transfer resistance decreased (3-9% of initial value) during the early stages of all except two of the experiments. Subsequent to this period, heat transfer resistance increased substantially with biofilm thickness as indicated in Fig. 8. Heat transfer resistance increased more

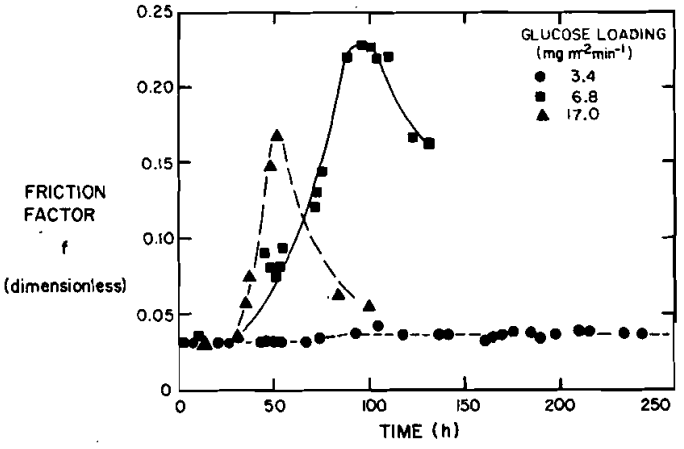

Figure 7 Influence of glucose loading rate on friction factor increase.

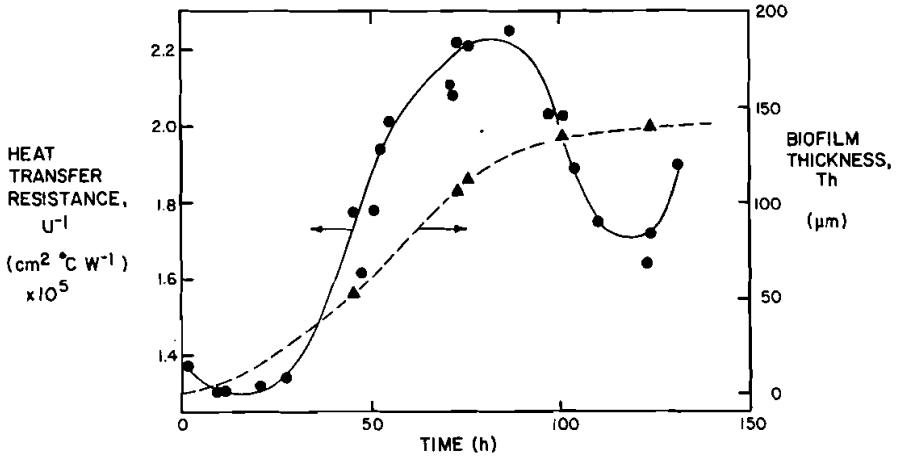

Figure 8 Progression of biofilm thickness and heat transfer resistance during a typical experiment.

rapidly in experiments with higher glucose loading rates (Fig. 9). Heat transfer resistance exhibited the same dramatic decrease as was observed with friction factor in certain experiments.

DISCUSSION

These experiments were conducted to determine the influence of biofilm formation on heat transfer resistance. A laboratory apparatus was constructed to simulate biofilm development in a heated tube as might occur in a condenser or heat exchanger.

Limitations of Reported Results

Several fundamental limitations must be considered when attempting to apply these results to biofouling in condensers or heat exchanges:

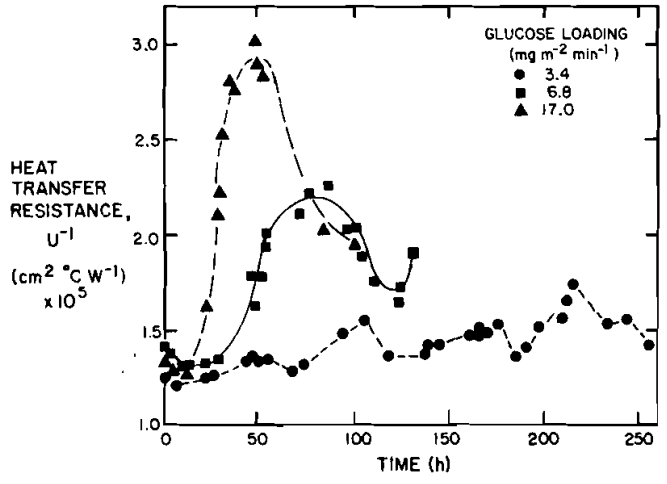

Figure 9 Influence of glucose loading rate on heat transfer resistance during a typical experiment.

1. A soluble substrate (glucose) was used as the sole energy source for microbial growth. Cooling waters most likely contain more complex carbon and energy sources. Consequently, microbial growth processes will probably be slower in real systems. Furthermore, the carbon and energy sources will be site-specific.
2. The microbial inoculum for all laboratory experiments was composed of a variety of microbial species. Use of a single substrate, however, essentially precludes the maintenance of a stable, mixed population. Therefore, as an experiment progressed, the microbial population was probably dominated by a very few species which could compete better for the available nutrients under the imposed experimental conditions. Microbial population diversity in cooling waters will be site-specific.
3. The feedwater in this research contained less than 1 mg/L of inert suspended solids. Suspended solids in cooling waters can increase or decrease deposition in a heated tube. Therefore, the actual phenomenon is more complex than what is presented here.
4. Within the experimental apparatus, a stainless-steel tube was used for pressure drop measurement and biofilm samples, while the test heat exchanger was aluminum.

Heat Transfer Resistance

Heat transfer resistance can be considered the sum of the convective heat transfer resistance and the conductive heat transfer resistance, as suggested previously by Eq. (2):

$$U_{\text{calc}}^{-1} = \frac{1}{h} + \frac{r_I \ln (r_1/r_I)}{k_B} + \frac{r_I \ln (r_i/r_1)}{k_{\text{tube}}} \qquad (2)$$

Overall heat transfer resistance = convective heat transfer resistance + conductive heat transfer resistance in the biofilm + conductive heat transfer resistance in the tube

In these experiments, U_{meas}^{-1} was determined directly from temperature measurements within the thick-walled heat exchanger. However, friction factor and biofilm thickness measurements permit determination of U_{calc}^{-1}, since

$$h = 0.125 f C_p^{0.33} \mu^{-0.67} k^{0.67} \rho v_m \qquad (6)$$

and

$$r_I = r_1 - Th \quad \text{and} \quad k_B = k$$

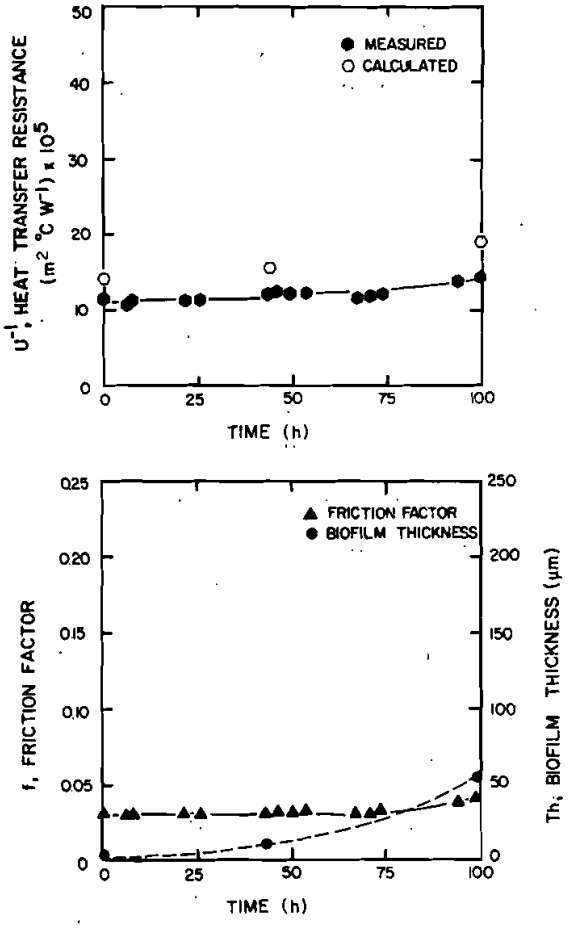

Figure 10 Comparison of measured and calculated values for heat transfer resistance at glucose loading rate = 3.4 mg m^{-2} min^{-1}.

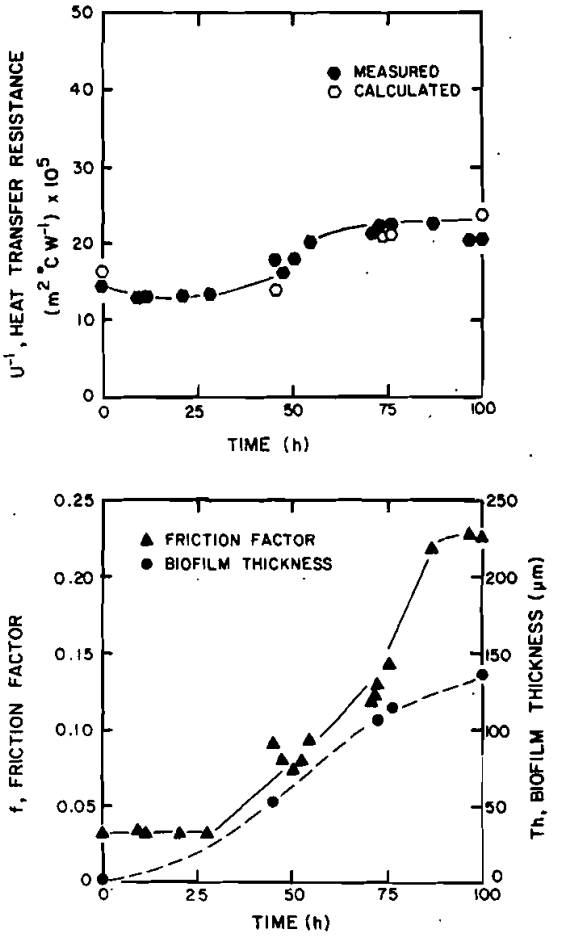

Figure 11 Comparison of measured and calculated values for heat transfer resistance at glucose loading rate = 6.8 mg m^{-2} min^{-1}.

Therefore,

$$U_{\text{meas}}^{-1} = (T_i - T_b) - \frac{r_2 q_2}{k_{\text{tube}}} \ln \left(\frac{r_i}{r_1} \right) \frac{r_1}{r_2 q_2} \qquad (14)$$

and U_{calc}^{-1} is described by Eq. (2).

Figures 10, 11, and 12 compare U_{meas}^{-1} and U_{calc}^{-1} from three experiments at different substrate loadings. U_{calc}^{-1} is determined by assuming the following:

1. The Colburn analogy is valid [Eq. (6)].
2. Biofilm thermal conductivity is equal to that of water at the same temperature ($k_B = k$).

In most cases, U_{calc}^{-1} is a good estimate of U_{meas}^{-1}. There were notable exceptions:

1. During the initial or induction period of the experiment when friction factor remains constant.
2. Following a dramatic decrease in U_{meas}^{-1} and f when a mature biofilm is present.

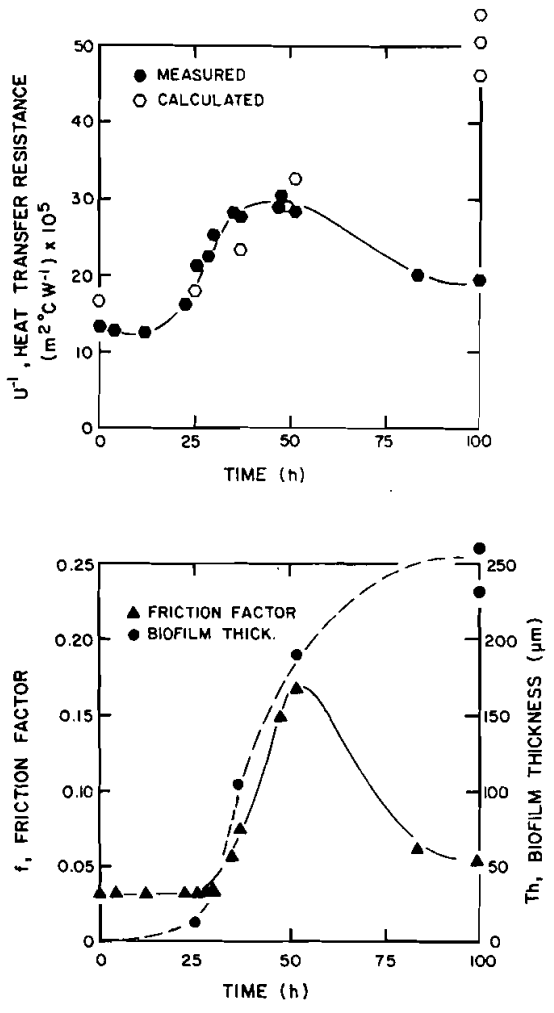

Figure 12 Comparison of measured and calculated values for heat transfer resistance at glucose loading rate = 17.0 mg m^{-2} min^{-1}.

Induction Period

During the induction period, biofilm thickness is small and the "hydraulic" roughness it effects cannot be detected by pressure drop measurements. Picologlou et al. [1] indicate that no measurable change in frictional resistance will occur until the biofilm thickness approaches the viscous sublayer thickness. In these experiments, the viscous sublayer thickness was 44 μm as calculated from conventional equations for turbulent tube flow. Figure 13 indicates that the critical biofilm thickness (Th_c) for changing frictional resistance was from 30 to 60 μm. Other data [9] presented in Fig. 14 further demonstrate the critical biofilm thickness concept.

When biofilm thickness Th is less than the viscous sublayer thickness, U^{-1}_{calc} and U^{-1}_{meas} are dramatically different. Figure 15 compares U^{-1}_{calc} and U^{-1}_{meas} during the initial period of a typical experiment. Time-smoothed biofilm thickness values have been used for U^{-1}_{calc}. The discrepancy between U^{-1}_{calc} and U^{-1}_{meas} is large prior to observing a friction factor increase. Subsequent to a friction factor increase, the U^{-1}_{calc} and U^{-1}_{meas} are essentially equal. One possible explanation of this is that roughness caused by the biofilm (when $Th < Th_c$) increases the convective heat transfer before the biofilm causes a change in friction factor. Further evidence for this effect is the observed decrease in U^{-1}_{meas} in the early stages of the experiment. Even if there were no increase in conductive resistance due to biofilm development, U^{-1}_{meas} should remain constant until the friction factor changes.

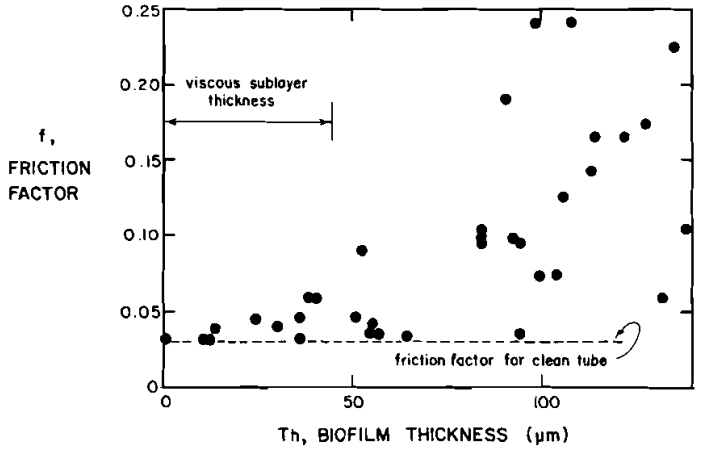

Figure 13 Influence of biofilm thickness on friction factor, indicating negligible change in f when $Th <$ viscous sublayer thickness. Data collected from all experiments are plotted (glucose loading rate varied from 3.4 to 17.0 mg m^{-2} min^{-1}).

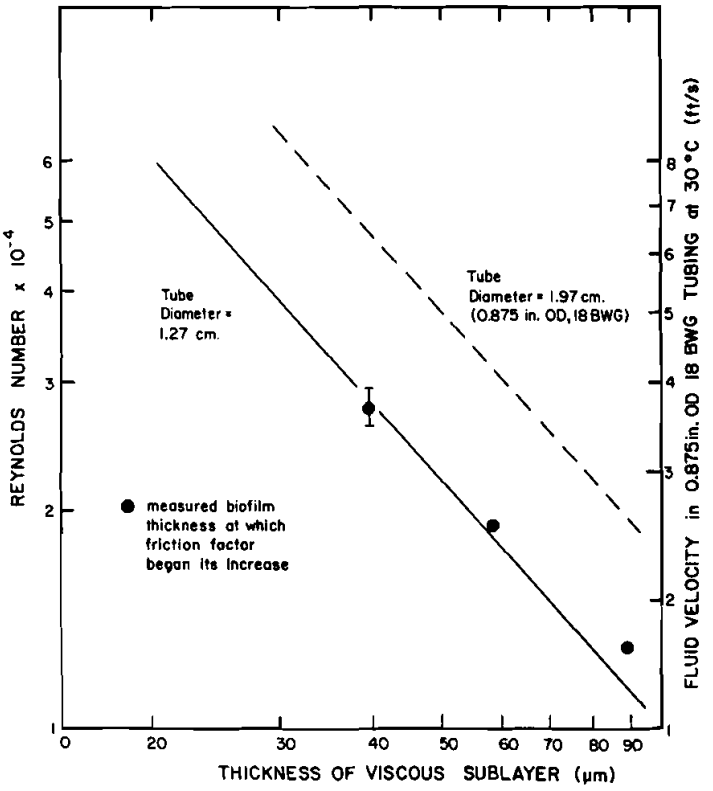

Figure 14 Influence of Reynolds number on thickness of the viscous sublayer. Circles indicate predicted viscous sublayer thickness based on measured biofilm thickness.

Mature Biofilms

In several experiments, a dramatic decrease in heat transfer resistance and frictional resistance were observed without a decrease in biofilm thickness (Fig. 12). Possible explanations for this behavior include the following:

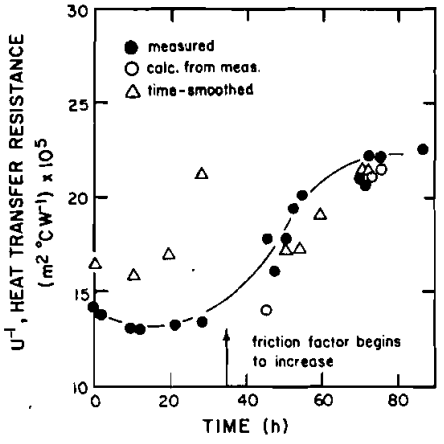

Figure 15 Comparison between measured and calculated heat transfer resistance, indicating large discrepancy during period when friction factor remains constant (biofilm thickness < viscous sublayer thickness).

1. Tube-wall temperature increased causing changes in biofilm properties which changed U^{-1} and f. In experiment 7, wall temperature was initially 34.7°C and increased to 44.0°C when U^{-1} was at its maximum. The increase in wall temperature may cause changes in the microbial population within the biofilm and/or the chemical properties of the biofilm.
2. Events occurring in the aluminum heat exchanger were not duplicated in the stainless-steel sections in which friction factor was measured and biofilm thickness determined.

Influence of Substrate Loading

Other investigators have measured the influence of biofilms on heat transfer resistance. The data are generally expressed in terms of the fouling factor, R_f, which is defined as follows:

$$R_f = U^{-1} - U_0^{-1} \tag{16}$$

where

U_0^{-1} = initial convective heat transfer coefficient $(Mt^{-3}T^{-1})$

R_f = fouling factor (t^3TM^{-1})

The data from two field investigations [3, 12] were chosen for comparison to R_f values calculated from data presented in this paper. Both studies were accomplished in seawater where microbial nutrient concentrations are low and biofilm development occurs at a low rate. Stumm and Morgan [13] indicate that organic carbon concentration in the oceans range from 0.5 to 1.2 mg/L. Higher concentrations would be measured in estuarine waters. Organic carbon concentrations entering the experimental system ranged from 4 to 80 mg/L resulting in organic carbon loadings in the range of 2.7 to 55 $mg\,m^{-2}\,min^{-1}$. Glucose carbon represented approximately one-half the organic carbon entering the system.

Figure 16 clearly indicates the significant influences of substrate loading on the rate of increase in heat transfer resistance. At very high loadings, the rate will probably either level off or decrease.

SUMMARY AND RELEVANCE TO PRACTITIONERS

Fouling refers to the formation of inorganic and/or organic deposits on surfaces. These deposits can impede the flow of heat across the surface, increase the rate of corrosion at the surface. Four types of fouling, and their combinations, may occur in heat exchangers:

1. Crystalline fouling–precipitation of inverse solubility scales (e.g., $CaCO_3$, $CaSO_4$) on the heated tube surface
2. Corrosion fouling–corrosion of tube metal which results in insulating layers of oxides on the tubes
3. Particulate fouling–attachment of particulate material on the tube surfaces
4. Biological fouling–formation of biological deposits on the tube surfaces

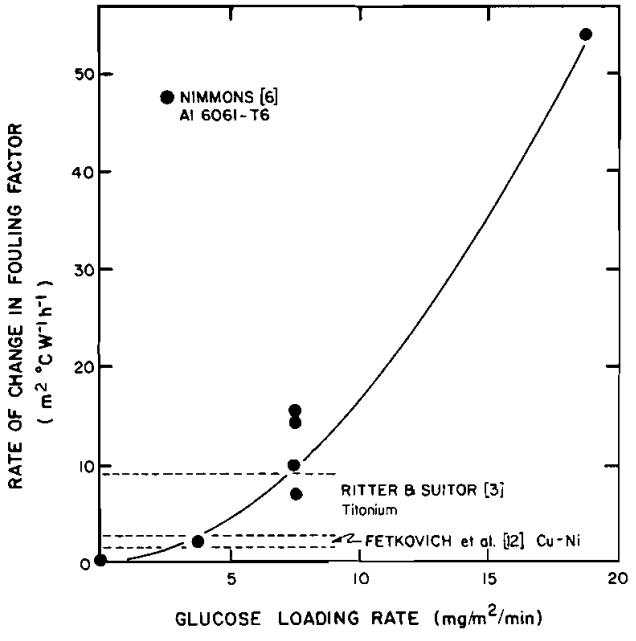

Figure 16 Influence of glucose loading rate on rate of increase in fouling factor (R_f). Ritter and Suitor [3] data obtained at $v_m = 0.6$–$1.2\ m\,s^{-1}$ and $T_1 = 26$–$38^\circ C$. Fetkovich et al. [12] data obtained at $v_m = 0.9$–$1.8\ m\,s^{-1}$ and $T_1 = 21^\circ C$. Nimmons [6] data obtained at $v_m = 0.8\ m\,s^{-1}$ and $T_1 = 39$–$45^\circ C$.

Biological fouling, or biofouling, is perhaps the least understood of the fouling processes. Some of the confusion regarding biofouling undoubtedly arises because of the interaction of several of the fouling processes (e.g., scaling, corrosion) at a given plant location. There can be no doubt that fouling biofilms that form on surface condensers reduce heat transfer and lower plant efficiency. The most common method of controlling biofilm accumulation is periodic chlorination. Chlorine dosage and application schedule are typically governed by observation of plant steam back pressure or operator experience. Recently, concern over toxicity from hypochlorous acid, or its reaction products, has resulted in federal regulations that limit the allowable concentrations of free available chlorine in cooling water discharges. The impact of the limitations is unknown but will vary significantly with location. At present, there is no sound basis for assessing the impact of these regulations.

This research work stemmed from the apparent need for a better basic understanding of fouling biofilm development and its influence on heat transfer so that the impact of these new regulations on power plant and industrial operations could be evaluated. The results from this study indicate the following:

1. Biofilm thermal conductivity is not significantly different from the thermal conductivity of water.
2. Biofilm development influences conductive and convective heat transfer. Both can be measured.
3. The influence of biofilm development on heat transfer can be described adequately if the following quantities are known: (a) biofilm thickness, (b) friction factor, (c) bulk water temperatures, and (d) wall temperature. One important restriction is that the biofilm thick-

ness be greater than the viscous sublayer thickness calculated for the clean tube.

4. Using the above conclusions, a fouling monitor can be constructed to provide instantaneous data on the extent of fouling and fouling deposit composition. This work is underway [14].
5. Substrate loading rate clearly influences the rate of increase in heat transfer resistance. Clearly, a nutrient-rich cooling water will result in higher fouling rates. In recirculating cooling water systems, organic and inorganic nutrients are concentrated and provide a rich growth environment for biofilms.

In other publications [10, 15, 16, 9], the influence of environmental factors on biofilm development, and its influence on frictional resistance, have been described based on laboratory results. Environmental factors considered include substrate loading, fluid shear stress, bulk water temperature, and wall temperature.

Clearly, other environmental factors may influence fouling and its effect on energy losses. Condenser tubes become rough after a period of service as a result of corrosion, erosion, and scaling. The increased roughness intensifies the influence of biofilms on frictional resistance [1]. Does this mean that certain condenser tube designs for enhanced heat transfer will result in amplified fouling?

Particulate material has been implicated as the cause of increased biofouling in some instances and has provided a measure of biofouling control in other cases [17]. The effect of inert particulate concentration and particle characteristics (e.g., specific gravity, size, composition) on biofouling must be determined.

It is postulated that chemical species such as calcium, magnesium, and silica are believed to influence the extracellular polymer matrix which is responsible for holding the biofilm together. Magnesium has been reported to play an important role in filament formation in attached growths. The effects of these constituents on biofilm properties and biofilm development rates must be determined, especially since chelants (e.g., EDTA, NTA) have been observed to be effective in partially removing biofilm from surfaces [9].

In recirculating cooling systems, pH and total dissolved solids (TDS) are controlled at levels set by consideration of corrosion and scaling. In addition, cycles of concentration, which affect TDS, are selected independently of biofouling considerations. Both pH and TDS may affect biofouling rates and biofouling control effectiveness. In zero discharge recirculating cooling tower systems, the problem is more acute. Organics are concentrated to very high levels increasing biofouling which requires large quantities of chlorine for control. Chlorine is reduced to chlorides which further increase TDS levels and corrosion rates.

Much effort at the plant level has been directed to enumerating and identifying specific organisms responsible for biofouling without any conclusive evidence that number concentration or population distribution reflect changes in heat transfer. Others have shown, however, that filamentous organisms in biofilm cause significantly greater frictional resistance than biofilms without filaments [1, 15]. Can more specific biofouling control measures be developed which only affect the nuisance organisms responsible for energy losses? Some progress is evident. Takiguchi et al. [18] have isolated compounds which specifically inhibit filamentous organism growth at concentrations less than 1 mg/L. The compounds showed no inhibitor activity against other bacteria, even at 100–200 mg/L.

Finally, results from this study indicate that fouling can be measured accurately by instruments that simulate the plant environment. The output from such instruments provide valuable information to the operating engineer regarding the extent of fouling which also reflects upon the performance of chemical treatment programs.

NOMENCLATURE

A_I	$2\pi r_I L$ (L^2)
C_p	specific heat of the liquid $(L^2 t^{-2} T^{-1})$
f	friction factor, $2d\,\Delta p/L\rho v_m^2$ (dimensionless)
$f_{\max}$	maximum friction factor attained (dimensionless)
F_D	dilution or feed flow rate $(L^3 t^{-1})$
F_R	recycle flow rate $(L^3 t^{-1})$
h	convective heat transfer coefficient at r_I $(Mt^{-3} T^{-1})$
k	fluid thermal conductivity $(MLt^{-3} T^{-1})$
k_B	apparent thermal conductivity of biofilm $(MLt^{-3} T^{-1})$
k_{tube}	thermal conductivity of tube wall material $(MLt^{-3} T^{-1})$
L	length of heat exchanger tube (L)
Pr_f	Prandtl number, $C_p\mu/k$ (dimensionless)
q_r	heat flux in $-r$ direction (Mt^{-3})
q_2	heat flux at r_2 (Mt^{-3})

Q heat transfer rate into the bulk fluid (ML^2t^{-3})
r radial distance (L)
r_1 inner radius of tube (L)
r_2 outside radius of tube (L)
r_i radial distance to inner thermistor of TWHE (L)
r_{ii} radial distance to outer thermistor of TWHE (L)
r_I radial distance to the biofilm (L)
R_G glucose removal rate ($ML^{-2}t^{-1}$)
R_f fouling factor (t^3TM^{-1})
St_b Stanton number, $h/C_p\rho v_m$ (dimensionless)
T_1 temperature at r_1 (T)
T_i temperature in the tube wall at r_i (T)
T_{ii} temperature in the tube wall at r_{ii} (T)
T_b bulk fluid temperature (T)
Th biofilm thickness, $r_1 - r_I$ (L)
Th_{max} maximum biofilm thickness attained (L)
T_I temperature at r_I (T)
U overall heat transfer coefficient ($Mt^{-3}T^{-1}$)
U_{calc} U calculated from Eq. (2) ($Mt^{-3}T^{-1}$)
U_{meas} U measured in TWHE ($Mt^{-3}T^{-1}$)
U_0 U in clean tube ($MT^{-3}T^{-1}$)
v_m mean fluid velocity (Lt^{-1})
z axial distance through the tube (L)
Δp pressure drop across length L ($ML^{-1}t^{-2}$)
μ fluid viscosity ($ML^{-1}t^{-1}$)
ρ fluid density (ML^{-3})
ρ_f biofilm density (ML^{-3})

REFERENCES

[1] Picologlou, B. F., Zelver, N., and Characklis, W. G., Biofilm Growth and Hydraulic Performance, *J. Hyd. Div.*, ASCE, vol. 106, no. HY5, p. 733, 1980.

[2] Purkiss, B. E., *Biotechnology of Industrial Water Conservation*, M&B Monographs, Mills and Boon, London, 1972.

[3] Ritter, R. B. and Suitor, J. W., Fouling Research on Copper and Its Alloys—Seawater Studies, HTRI Progress Rept., INCRA Project No. 214A, April 1976.

[4] Kirkpatrick, J. P., McIntire, L. V., and Characklis, W. G., Mass and Heat Transfer in a Circular Tube with Biofouling, *Water Research*, vol. 14, p. 117, 1980.

[5] Colburn, A. P., A Method of Correlating Forced Convection Heat Transfer Data and a Comparison with Fluid Friction, *Trans. AIChE*, vol. 29, p. 174, 1933.

[6] Nimmons, M. G., Heat Transfer Effects in Turbulent Flow Due to Biofilm Development, M.S. thesis, Rice University, Houston, 1979.

[7] Characklis, W. G., Biofilm Development and Destruction in Turbulent Flow, *Ozone: Science and Engineering*, vol. 1, p. 167, 1979.

[8] Trulear, M. G. and Characklis, W. G., Dynamics of Biofilm Processes, 34th Ind. Waste Conf., Purdue Univ., Ann Arbor Science, p. 838, 1980.

[9] Characklis, W. G., Biofouling Film Development and Destruction, Electric Power Res. Inst., RP902-1, 1980.

[10] Zelver, N., Biofilm Development and Associated Energy Losses in Water Conduits, M.S. thesis, Rice University, Houston, 1979.

[11] Weast, R. C. (ed), *Handbook of Chemistry and Physics*, 51st ed., p. E-20, The Chemical Rubber Co., Cleveland, 1970.

[12] Fetkovich, J. G., Grannemann, G. N., Mahalingam, L. M., and Meier, D. L., Measurements of Biofouling in OTEC Heat Exchangers, *Proc. 5th OTEC Conference*, Miami, 1978.

[13] Stumm, W. and Morgan, J. J., *Aquatic Chemistry*, Wiley-Interscience, New York, 1970.

[14] Characklis, W. G., Zelver, N., Turakhia, M., and Nimmons, M. J., Fouling and Heat Transfer, accepted for presentation, ASME Heat Transfer Division, session on Fouling in Heat Exchange Equipment, *20th Natl. Heat Transfer Conf.*, Milwaukee, 1981.

[15] Trulear, M. G. and Characklis, W. G., Dynamics of Biofilm Processes, *J.W.P.C.F.*, accepted for publication.

[16] Stathopoulos, N., Influence of Temperature on Biofilm Processes, M. S. thesis, Rice University, Houston, 1981.

[17] Bour, D. P., Biofouling Experience and Practices on Once-Through Condensers at Electric Generation Stations, *Condenser Biofouling Control*, ed. J. F. Garey et al., pp. 267-277, Ann Arbor Science, Ann Arbor, 1980.

[18] Takiguchi, Y., Yoshikawa, H., and Terao, M., New Selective Growth Inhibitors of *Sphaerotilus natans*, Anslimins A and B, *Appl. Env. Microbiol.*, vol. 39, no. 6, pp. 1123-1128, 1980.

W. G. Characklis is Professor of Civil and Chemical Engineering at Montana State University. He received his B.E.S. in chemical engineering and Ph.D. in environmental engineering from Johns Hopkins University (1970) and M.S.Ch.E. from the University of Toledo. He has done research and consulting for the chemical process industries in the area of industrial water and wastewater. Until 1979 he was Professor of Environmental Engineering at Rice University. His research interests are in chemical and microbial process engineering.

Michael J. Nimmons graduated from Rice University with an M.S. in Environmental Science and Engineering and received undergraduate degrees in Philosophy and Environmental Engineering at St. John's College and Humboldt State University. Mr. Nimmons has assisted in the design of several water treatment systems for the mining and metallurgical industries. He is presently employed by D'Appolonia Consulting Engineers in process design and alternative technology development for hazardous waste disposal, water treatment, and hydrologic control facilities.

Basil F. Picologlou is a project manager at Argonne National Laboratory working in the field of magnetohydrodynamic electric power generation. He has a B.S. degree from the National Technical University of Athens and M.S. and Ph.D. degrees from Purdue University. He taught at Rice University from 1974 to 1979.